Nanostructured $Co_{1-x}Ni_x(Sb_{1-y}Te_y)_3$ skutterudites: Theoretical modeling, synthesis and thermoelectric properties

Christian Stiewe[a)]
German Aerospace Center (DLR), Linder Hoehe, 51147 Cologne, Germany

Luca Bertini
Istituto di Scienze e Tecnologie Molecolari (ISTM), Via Camillo Golgi 19, 20133 Milano, Italy

Muhammet Toprak
Royal Institute of Technology (KTH), Stockholm, Sweden

Mogens Christensen
University of Aarhus, Department of Chemistry, DK-8000 Aarhus C, Denmark

Dieter Platzek
German Aerospace Center (DLR), Linder Hoehe, 51147 Cologne, Germany

Simon Williams
NEDO Laboratory for Thermoelectric Engineering (NEDO), Cardiff, United Kingdom

Carlo Gatti
Istituto di Scienze e Tecnologie Molecolari (ISTM), Via Camillo Golgi 19, 20133 Milano, Italy

Eckhard Müller
German Aerospace Center (DLR), Linder Hoehe, 51147 Cologne, Germany

Bo B. Iversen
University of Aarhus, Department of Chemistry, DK-8000 Aarhus C, Denmark

Mamoun Muhammed
Royal Institute of Technology (KTH), Stockholm, Sweden

Michael Rowe
NEDO Laboratory for Thermoelectric Engineering (NEDO), Cardiff, United Kingdom

(Received 16 July 2004; accepted 30 November 2004; published online 28 January 2005)

The properties of Te-doped $Co(Sb_{1-y}Te_y)_3$ and Te-Ni double-doped $Co_{1-x}Ni_x(Sb_{1-y}Te_y)_3$ nanostructured skutterudites were evaluated by means of x-ray powder diffraction, and transport properties measured on the synthesized samples have been compared with *ab initio* theoretical modeling. Theoretical optimal dopant contents have been evaluated according to the maximum value of the power factor, calculating the electronic transport properties from the *ab initio* material band structure using semiclassical Boltzmann transport theory. The samples have been synthesized by chemical alloying with Te substitution for Sb up to 2.5 at. % and Ni substitution for Co up to 2.0 at. %. X-ray powder diffraction has been performed on all samples to reveal information about phase purity and Rietveld refinement was performed for the phase composition and cell parameter. The thermoelectric properties of the resulting consolidates were investigated in a temperature range from 300 to 723 K using various measurement facilities. A standardization and round robin program was started among the participating evaluation laboratories in order to ensure reliability of the data obtained. The significant reduction in thermal conductivity, when compared to highly annealed $CoSb_3$, could be proved which is caused by the nanostructuring, resulting in a high concentration of grain boundaries. A combination of substitution levels for Ni and Te has been found resulting in the largest *ZT* value of 0.65 at 680 K among unfilled skutterudite materials. © *2005 American Institute of Physics*. [DOI: 10.1063/1.1852072]

I. INTRODUCTION

The performance of thermoelectric materials is usually evaluated in terms of their dimensionless thermoelectric figure of merit $ZT=(S^2\sigma/\kappa)T$, where S is the Seebeck coefficient, σ the electrical conductivity, $\kappa=\kappa_L+\kappa_e$ the total thermal conductivity with its lattice and electronic contributions, and T is the absolute temperature.

Materials of the skutterudite structure are very well known as promising candidates for high-performance thermoelectric applications within the phonon-glass-electron-crystal concept proposed by Slack,[1] because of the opportunity of reducing the material's high thermal conductivity by introducing guest atoms into the cage-like framework. The

[a)]Electronic mail: christian.stiewe@dlr.de

target is to lower the thermal conductivity to values close to that of amorphous material of the same stoichiometry.

This work is focused on the theoretical and experimental evaluation of the properties of Te substitution for Sb and its combination with Ni substitution for Co in $CoSb_3$ skutterudite as thermoelectric material.

$Co(Sb_{1-y}Te_y)_3$ and $Co_{1-x}Ni_x(Sb_{1-y}Te_y)_3$ $(0 \leqslant x,y \leqslant 1)$ are the Te-doped and the Te-Ni double-doped systems, respectively, obtained from $CoSb_3$ binary skutterudite. The parent compound, $CoSb_3$, has a bcc structure with space group $Im\bar{3}$ and eight formula units in the primitive cell. Sb and Te atoms occupy $24g$ $(0,y,z)$ positions and form almost square D_{2h} pnicogen rings with general formula $Sb_{4-y}Te_y$ $(y=1-4)$. Co and Ni atoms sit in $8c$ $(\frac{1}{4},\frac{1}{4},\frac{1}{4})$ positions and form a simple cubic transition metal sublattice wherein six out of eight of the cubic voids are filled by the pnicogen rings. In filled systems selected atoms can occupy interstitial $2a$ (0,0,0) positions. It has been recently shown that neither Ni (Refs. 2 and 3) nor Te (Refs. 4 and 5) can occupy also interstitial positions.

The *n*-dopant Ni or Te atoms are known to have positive effects on the thermoelectric properties of $CoSb_3$.[6,7] In both cases the presence of a small amount of these two atoms brings in a decrease of the thermal conductivity and, at the same time, an increase of the power factor $S^2\sigma$. The idea of the double doping is the synergic combination of the beneficial effect of two types of dopant atoms, as recently shown by Dyck *et al.*[8] in the case of the Ba-Ni filled-doped skutterudite systems.

A recently developed chemical alloying approach[9] has been tuned for the fabrication of nanocrystalline $Co(Sb_{1-y}Te_y)_3$ and $Co_{1-x}Ni_xSb_{3-y}Te_y$ skutterudites. This approach has compromised solution chemical synthesis and thermochemical processing under controlled conditions. In order to reduce the heat transport already in the unfilled skutterudite, with only little or even no effect on the electrical conductivity, we tried to increase the concentration of grain boundaries by nanostructuring the basic material. This is achieved by very small particle sizes of the starting polycrystalline powders in the nanometer range, providing the chance of even further reduction in κ by filling the resulting structure. To overcome the loss of Sb during the preparation procedure, a specially designed furnace was constructed and used for calcination and reduction. Negative influences on the electrical conductivity are compensated for by doping the $CoSb_3$ based material with Ni (Ref. 10) or Te, or combinations of both. For the determination of the transport properties of the pressed pellets, various measurement devices were used, owned by the three participating evaluation laboratories. To ensure reliability and reproducibility of the data obtained, a program of standardization and round robin testing has been started with the aim to check self-built measurement facilities and to establish standard material for future calibration tests available for other European laboratories interested in this subject.

The theoretical part of this article is devoted to the prediction of the best Te, Ni, and combined Te-Ni doping levels according to the power factor $S^2\sigma$. The resulting improvement of the total figure of merit is estimated through the electronic figure of merit $Z_eT=T(S^2\sigma/\kappa_e)$. Electronic transport properties are calculated within semiclassical Boltzmann transport theory in the constant relaxation time approximation. According to this theory, the electronic transport properties are derived from material's electronic structure alone, which is calculated by means of *ab initio* electronic structure calculations performed by using the density functional theory (DFT) approach.

II. THEORETICAL AND COMPUTATIONAL DETAILS

Fully periodic *ab initio* calculations were performed using CRYSTAL98[11] code. A generalized gradient approximation DFT approach was adopted using the B3PW91[12] functional and Hay-Wadt pseudopotentials[13,14] (PP). Small-core PP for Co and Ni atoms (17 and 18 active electrons, respectively) and large-core for Sb and Te atoms (5 and 6 active electrons, respectively) were selected. Starting from the double-ζ Gaussian basis[15] sets relative to these PP, a new double-ζ basis set was generated by cutting the most diffuse functions from the outer shells and by modifying the remaining functions and contraction coefficients so as to preserve the original atomic shell Mulliken populations, in the case of the isolated atoms. The $s=p$ constraint was imposed on the exponent of the most diffuse shell of the Sb and Co atoms, in order to save computational time. All calculations were carried out in the $Im\bar{3}$ space group, with Sb (Te) atoms at the $24g$ and Co (Ni) at the $8c$ special positions. For each system the structural parameters were optimized against total energy using the LoptCG script[16] and retaining $Im\bar{3}$ space group. The optimized parameters were therefore the two fractional coordinates of the $24g$ position and the cell parameter. We estimated the electronic transport properties using the ELTRAP[17] code, interfaced with CRYSTAL98 calculation package and implementing the semiclassical Boltzmann's transport theory[18] in its monoelectronic formulation and in the approximation of a constant relaxation time τ.[19] The frozen band approximation of the Boltzmann theory accounts for the actual doping level by filling or emptying out the electronic bands of the reference system. In this way we can avoid the calculation of the band structure at the actual doping level, that would imply large supercell computations which are extremely CPU demanding. In a recent paper,[20] we found that electronic transport properties for doped skutterudite systems calculated within the Boltzmann theory and the frozen band approach are in good agreement with measured ones. In our case, we adopt the $Co_3NiSb_{11}Te$ band structure as reference, while usually it has been used the Co_4Sb_{12} one. The advantage is that of taking explicitly into account the modification of the bands due to the presence of the dopant atoms.

Seebeck coefficient **S**, the electrical conductivity σ, and the electronic contribution to the thermal conductivity κ_e are all second-rank tensors whose isotropic part (S, σ, and κ_e) is given as $1/3$ of their trace. Integrals over the first Brillouin zone were evaluated numerically by sampling the band structure $E_n(\mathbf{k})$ and using an equally spaced cubic grid with a total of 40^3 k-points for each n band.[19] Using a constant relaxation time, the Seebeck coefficient turns out to be τ independent,

TABLE I. Nominal composition of investigated $CoSb_3$ samples doped with Ni and Te with the atomic dopant percentage, the corresponding XRD cell parameters in Å, the Hall carrier concentrations in 10^{20} cm^3, and the transport properties (Seebeck coefficient in $\mu V/K$, electrical conductivity σ in S/cm, and total thermal conductivity κ in W/mK) at 300 K.

	Te, Ni (at. %)	*a*-XRD	Carr. conc.	*S*	σ	κ
$CoSb_{2.97}Te_{0.03}$	0.75, 0	9.0306(2)	0.053	−241.4	257	5.0
$CoSb_{2.96}Te_{0.04}$	1.0, 0	9.0423(2)	0.083	−235.6	237	4.6
$CoSb_{2.91}Te_{0.09}$	2.25, 0	9.0361(2)	0.16	−203.2	220	3.9
$Co_{0.92}Ni_{0.08}Sb_{2.97}Te_{0.03}$	0.75,2.0	9.0355(2)	0.67	−130.8	681	4.7
$Co_{0.92}Ni_{0.08}Sb_{2.91}Te_{0.09}$	2.25,2.0	9.0372(2)	1.1	−102.9	794	4.1

while σ and κ_e depend linearly on τ, which is generally unknown. The best *n*-doping level can be estimated by maximizing $S^2\sigma$ versus *n*, whereas the resulting improvement on *ZT* cannot be evaluated, being $S^2\sigma$ scaled by τ. We thus introduced the relaxation-time-independent electronic figure of merit $Z_eT=T(S^2\sigma/\kappa_e)$ as an upper bound to the total figure of merit *ZT*. This quantity is τ independent only when the two relaxation times—that for the electric current and that for the thermal current—are equal. Due to this, Z_eT is conveniently used to estimate *ZT* only once the optimal doping level has been obtained from $S^2\sigma$.

III. SYNTHESIS

The composition of the samples synthesized is reported in Table I. A chemical alloying route has been used for the synthesis of nanocrystalline skutterudites. Using in-house (KTH) developed computer software and database for chemical equilibrium modeling, the multicomponent system consisting of H^+-Co^{2+}-Ni^{2+}-Sb^{3+}-Te^{4+}-$C_2O_4^{2-}$-Cl^--NH_3-H_2O has been extensively studied to determine the optimal preparation conditions for coprecipitation of the precursor powders with the required stoichiometry. An optimal *p*H range of 1–3 has been determined so that all of the desired metal components of $Co_{1-x}Ni_xSb_{3-y}Te_y$ precipitate completely when the ratio of their concentrations in the solution is kept in the stoichiometry. Figure 1 presents a general scheme of the chemical alloying process used in this work.

Fabricated nanostructured skutterudite materials were kept under hexane during transport and handled in a glovebox under nitrogen atmosphere to avoid the oxidation of the powders. Pellets for evaluation of the thermoelectric properties were produced by hot uniaxial pressing of the powders at 853 K under 100 MPa for 30 min.

Scanning electron microscopy (SEM) investigations reveal the coprecipitated powder as rod-like particles of a few micrometers in length and submicrometers in diameter with some agglomeration. After calcination, the particles brake down to smaller sizes as rock-like with less agglomeration. The final alloy powder is much smaller in size than the cross-lined nanoparticles.

Detailed investigation by transmission electron microscopy (TEM) reveals a clear morphology of the alloyed sample as spherical nanoparticles of 10–20 nm in diameter (Fig. 2). Hot pressing of these materials led to grain sizes in the range of 150–250 nm, because of sintering processes. All consolidated samples exhibit densities between 7.13 and 7.41 g/cm^3, which is 93%–97% of the x-ray density (7.64 g/cm^3).[21]

IV. MATERIALS CHARACTERIZATION

X-ray powder diffraction analysis (XRD, Philips PW 1012/20 and Stoe powder diffractometer equipped with Cu tube, curved graphite monochromator, and Ni filter to suppress fluorescence placed in front of the position sensitive detector) has been performed at different processing stages to

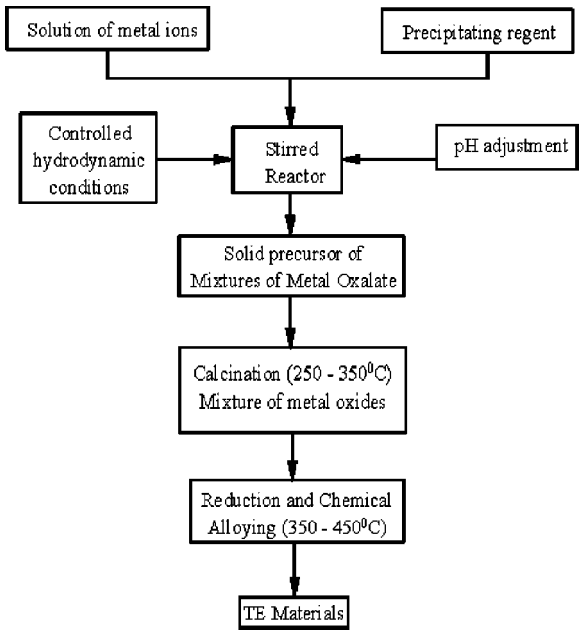

FIG. 1. A general schematic presentation of the chemical alloying approach.

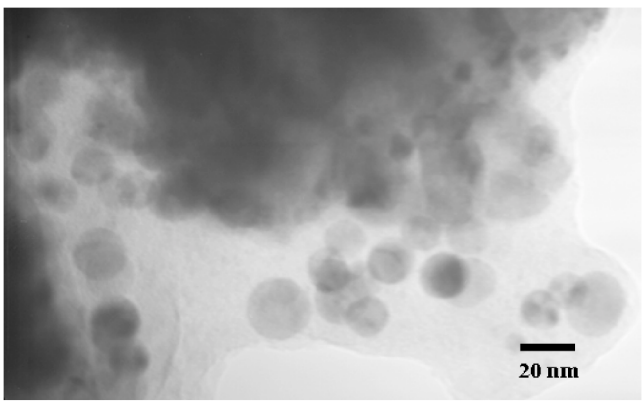

FIG. 2. TEM micrograph of skutterudite powder.

TABLE II. Optimized values (Å) for the cell parameter a, the fractional coordinates, y and z, of atoms at 24g special position. Fermi level (FL) energies in Hartree. Electron populations P_e (electrons) computed from the total 1-density matrix projected on the energy interval between the Fermi level of the investigated systems and the top of the valence band in $CoSb_3$. The calculated σ values ($\tau=10^{-14}$ s) at 300 and 700 K are in (S/cm) $\times 10^{-5}$. Transport properties for $Co_{0.75}Ni_{0.25}Sb_{2.75}Te_{0.25}$ are calculated with an n-doping level adjusted to 0.25 electrons cell respect to $CoSb_3$.

						σ	
MX_3	a	y	z	FL	P_e	300 K	700 K
$CoSb_3$[a]	9.1823	0.3308	0.1594	−0.1330			
$CoSb_{2.75}Te_{0.25}$[b]	9.1970	0.3310	0.1592	−0.1090	0.25	0.99	0.93
$Co_{0.75}Ni_{0.25}Sb_3$[c]	9.2101	0.3315	0.1592	−0.1147	0.26	1.6	1.5
$Co_{0.75}Ni_{0.25}Sb_{2.75}Te_{0.25}$	9.2210	0.3315	0.1592	−0.1165	0.50	1.1	1.0

[a]Reference 4.
[b]Reference 5.
[c]Reference 2.

evaluate the mechanism of synthesis and to investigate the phase purity of materials. SEM (Jeol JSM-840) has been used to investigate the morphology and size of obtained nanostructured materials at different processing stages. TEM (Jeol-2000EX) has also been performed for further study of the particle size distribution. Atomic force microscopy (AFM, Nanoscope IIIa) has been used in the tapping mode for the study of microstructure of hot-pressed powders.

XRD revealed a purity of the desired phase with impurities up to 4%, which are identified as $CoSb_2$ and pure Sb phases. In Table I, the experimental XRD cell parameters are reported. No clear dependence of the lattice parameter on the nominal doping level was found. Since from theory, the substituting Te is not expected to affect the lattice parameter,[2,5] the observed variation of a is likely a result of the integrational measurement and the additional phases of $CoSb_2$ and Sb. When nanostructured materials are designed, the control of the actual doping level and the phase purity is less effective. In case of the $CoSb_{2.97}Te_{0.03}$ sample an additional Te phase of 0.15 at. % might explain the measured unusual low lattice parameter by incomplete substitution for Sb. In addition, Wojciechowski *et al.*[22] reported a solubility limit of Te in $CoSb_3$ of 1.5 at. %. Excess Te might segregate in the sample instead of substituting for Sb, thus changing the measured lattice parameter as well. This way, the actual chemical composition might differ from the nominal one, but the dependence of the charge carrier concentration on the nominal doping level proves the given sequence.

V. COMPUTATIONAL RESULTS

Optimal structural parameters are listed in Table II for the investigated $Co_{1-x}Ni_xSb_{3-y}Te_y$ systems ($x=y=0$; $x=0$, $y=0.25$; $x=0.25$, $y=0$, $x=y=0.25$). Structural results for pure Te- and pure Ni- doped $CoSb_3$ systems have been reported earlier.[2,5] When Te, Ni, or a combination of both is introduced in the $CoSb_3$ frame, the cell parameter increases. The Te-Ni double-doped system exhibits a 0.4% increase, while the Te or Ni single-doped systems show a slightly lower cell expansion.

Total and atom projected density of states (DOS) for $Co_{0.75}Ni_{0.25}Sb_{2.75}Te_{0.25}$ are shown in Fig. 3. The Te and Ni states lie roughly in the same energy range of the states they replace. The $CoSb_3$ band gap width (0.65 eV) is narrowed to 0.1 eV. The Fermi level is shifted upward in energy yielding a heavily n-doped material and populating the first three $CoSb_3$ conduction bands. Similar behavior was reported earlier[2,4] for $CoSb_{2.75}Te_{0.25}$ and $Co_{0.75}Ni_{0.25}Sb_3$.

In Table II are reported the σ values ($\tau=10^{-14}$ s) at 300 and 700 K, while Fig. 4 shows Seebeck coefficient values as a function of the temperature. All data refer to a carrier concentration adjusted to 0.25 electrons/cell respect to undoped

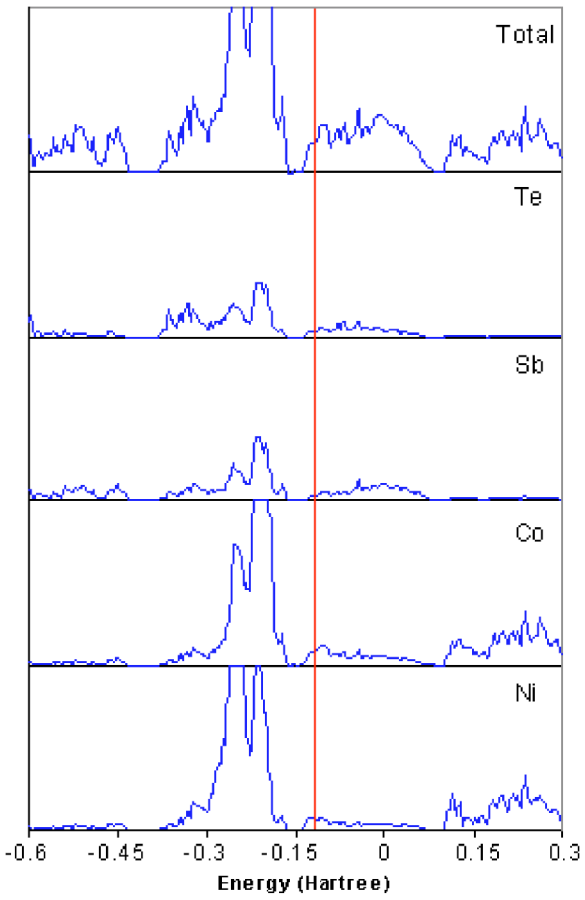

FIG. 3. $Co_{0.75}Ni_{0.25}Sb_{2.75}Te_{0.25}$ total and atom projected DOS. The vertical line refers to the Fermi energy level.

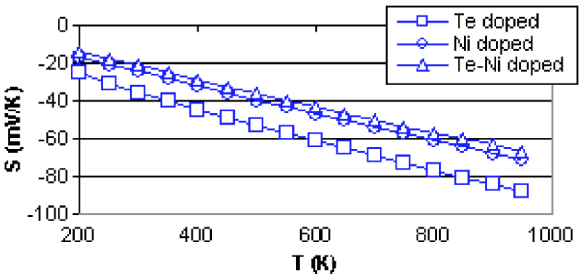

FIG. 4. The calculated Seebeck coefficients for $CoSb_{2.75}Te_{0.25}$, $Co_{0.75}Ni_{0.25}Sb_3$, and 0.25 electrons/cell *p*-doped $Co_{0.75}Ni_{0.25}Sb_{2.75}Te_{0.25}$.

$CoSb_3$. The σ values increase almost linearly with increasing dopant content and are scarcely temperature dependent, with highest values for Ni doped system. In order to rationalize this best performance for Ni, we calculated the rms velocity $\sqrt{\langle v^2\rangle_n}$ of the bands around Fermi level given by

$$\sqrt{\langle v^2\rangle_n} = \sqrt{\frac{1}{3}(\langle v_x^2\rangle_n + \langle v_y^2\rangle_n + \langle v_z^2\rangle_n)},$$

$$\langle v_x^2\rangle_n = \frac{1}{N_k}\sum_{i=1}^{N_k} v_{n,i}^2,$$

where $v_{n,i}(k_i) = (1/\hbar)\partial E_n(\mathbf{k})/\partial k_i$ is the *n*-band velocity in the *i*th direction ($i = x, y, z$), N_K is the number of *k*-points used to sample this band along the *i*th direction and $v_{n,i}^2$ is its squared velocity at point k_i. In Table III are reported the rms band velocities for the three bands that mostly contribute to the transport properties, along with $CoSb_3$ values for the sake of comparison. On average, the values of $\sqrt{\langle v^2\rangle_n}$ for Ni-doped system are 25% larger than in Te-doped system, and if Ni is added to these latter, $\sqrt{\langle v^2\rangle_n}$ increases of about 10%. Overall, Ni seems to be a better dopant atom as for the electrical conductivity enhancement.

The calculated trends for *S* are quite similar to each other, with negative *S* values at each *T* and magnitudes that increase almost linearly with *T*. At a given temperature, *S* magnitudes decrease with increasing dopant content. Figure 5 display trends for $S^2\sigma$ at 300 and 700 K as a function of the *n*-doping for the systems studied, with corresponding optimal doping levels are reported in Table IV. These levels are scarcely affected by *T* and are in the 0.08–0.15 electrons/cell range with respect to undoped $CoSb_3$. Optimal Te content in $CoSb_{3-x}Te_x$ is overestimated with respect to the experimental values[7] of 0.03–0.06, while experimental data for Ni optimal content in $Co_{3-x}Ni_xSb$ are not available. The Te-Ni optimal doping level is about 20% lower than the experimental one (0.11 electrons/cell). The

TABLE III. Rms band velocities of the first three unoccupied bands (UB) respect to $CoSb_3$. These bands give the dominant contribution to the electronic transport properties of the doped systems.

Band	$CoSb_3$	$Co_{0.75}Ni_{0.25}Sb_3$	$CoSb_{2.75}Te_{0.25}$	$Co_{0.75}Ni_{0.25}Sb_{2.75}Te_{0.25}$
UB	0.086	0.088	0.067	0.084
UB+1	0.071	0.11	0.089	0.098
UB+2	0.10	0.12	0.10	0.11

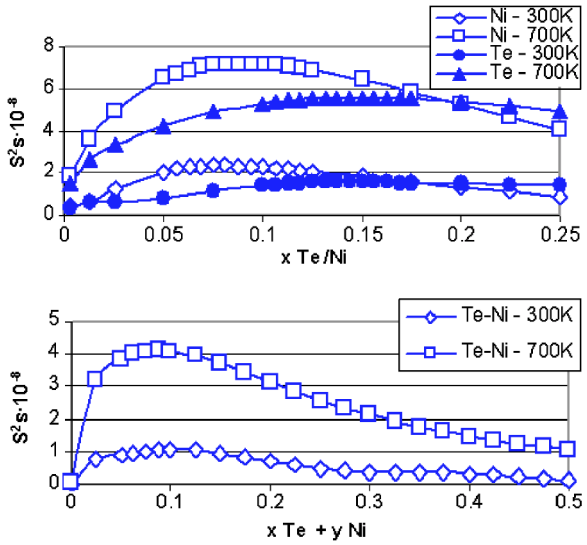

FIG. 5. $S^2\sigma$ at 300 and 700 K as a function of the Ni and Te content for $CoSb_{3-x}Te_x$ and $Co_{1-x}Ni_xSb_3$ with $0 \leqslant x \leqslant 0.25$, and $Co_{3-x}Ni_xSb_{3-x}Te_x$ with $0 \leqslant x+y \leqslant 0.5$.

Z_eT values at the highest *T* are similar to each other, indicating that the electronic transport properties adjust themselves so as to give similar thermoelectric behavior when an optimal quantity of substitutional *n*-dopant element is introduced in the $CoSb_3$ frame.

VI. MEASUREMENT STANDARDIZATION AND EVALUATION OF THE THERMOELECTRIC PROPERTIES

The need for ensuring accurate and consistent experimental data is crucial for the success of any materials development program. The use of different measurement techniques, sample geometrical requirements, and equipment, however, meant that some form of measurement standardization was necessary between partners, ensuring that meaningful and comparative data would result. For calibration of electrical resistivity and thermal diffusivity measurements, a suitable certified reference material (SRM1460) was obtained from NIST. Calibrations of Seebeck coefficient measurements were compared using both constantan alloy and palladium metal foil against literature values for these materials. Finally, round robin testing was made using skutterudite thermoelectric materials.[23]

All comparisons of the data obtained are within a range of 2%–3% maximum deviation, proving the reliability and accuracy of these measurements.

TABLE IV. Best doping level at 300 and 700 K, with corresponding $S^2\sigma$ and Z_eT values.

	300 K			700 K		
System	$x+y$	$S^2\sigma\times10^{-8}$	Z_eT	$x+y$	$S^2\sigma\times10^{-8}$	Z_eT
$CoSb_{3-x}Te_x$	0.144	1.57	0.85	0.150	5.55	2.26
$Co_{1-x}Ni_xSb_3$	0.081	2.34	1.20	0.088	7.15	2.49
$Co_{1-x}Ni_xSb_{3-y}Te_y$	0.10	1.05	0.70	0.088	4.11	2.23

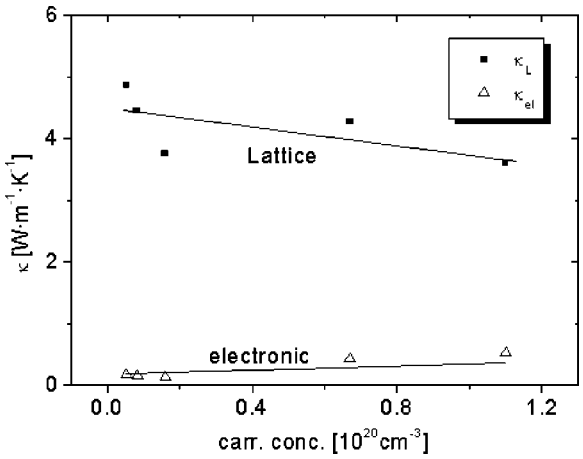

FIG. 6. Room-temperature thermal conductivity vs charge carrier concentration.

The temperature dependence of σ, κ, S, and ZT of the Ni- and Te-substituted nanomaterial were investigated in the range from room temperature up to 723 K, under vacuum using various partners' facilities.[24] These latter include mainly self-built devices, using four-point-probe technique for electrical conductivity measurement and applied temperature gradients for Seebeck coefficient investigation. Thermal conductivity has been calculated from measurements of the thermal diffusivity by a laser flash apparatus (Netzsch LFA 427 and self-built facility) and heat capacity has been determined by differential scanning calorimetry (Netzsch DSC 404 and Netzsch DSC 200).

Measurements of the Hall coefficient (see Table I) at room temperature gave information about the types of charge carriers and their concentrations. Figure 6 contains the dependence of the total thermal conductivity on the charge carrier density obtained by Hall measurements at room temperature. The separate electrical and lattice contributions were calculated using the Wiedemann–Franz law. The electrical part is about 10% of the total thermal conductivity and it increases only slightly with higher carrier density. This result ensures that the best doping levels predicted according to the recipe of maximum $S^2\sigma$ will be a good estimate of the corresponding experimental values. On the other hand, the lattice contribution is reduced slightly from 4.5 to $\sim$4.0 W/(m K) for higher carrier density, giving evidence of a raised electron-phonon scattering process. This value is still too large for a good thermoelectric material, and κ_L further reduction is necessary, for example, by optimizing the doping level and introducing rattling atoms.

In Fig. 7, the temperature dependence of the thermal and electrical conductivity, Seebeck coefficient, and figure of merit is displayed. The same data are also reported for $Co_{0.95}Ni_{0.05}Sb_3$ for the sake of comparison. The overall thermal conductivity ranged between 3.0 and 5.0 W/(m K) and exhibits a negative temperature dependence for all prepared doping combinations. The pure Te doping seems to have a positive effect, because of the 20% to 23% reduced κ values in the whole investigated T range for the maximum Te level compared to the lowest Te doping. Ni additon counteracts the effect of Te, resulting in a less reduced thermal conductivity.

The electrical conductivity changes with doping but is hardly temperature dependent. The largest σ values of $\sim$1000 $(\Omega\,\mathrm{cm})^{-1}$ were obtained for heavily doped systems and still show a positive T dependence, indicating semiconductor behavior. As an unexpected result, Te reduces the electrical conductivity of the non-Ni samples slightly, despite the increase in carrier concentration. This fact can probably be ascribed to the fluctuations of the samples grain size, because the electrical and thermal conductivity values are more sensitive to sample grain size than Seebeck coefficient

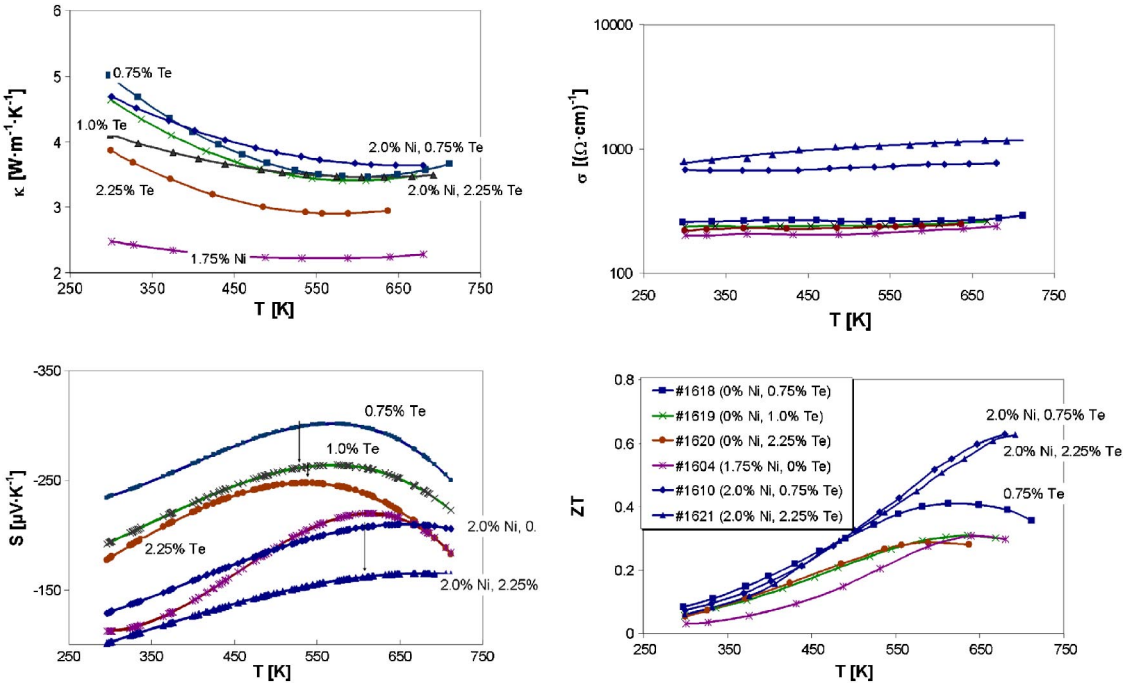

FIG. 7. Thermoelectric evaluation data on Ni- and Te-doped $CoSb_3$ skutterudites.

values.[25] For the Ni- doped samples, σ is increased by the Te addition. In both cases (Te increase at constant Ni and vice versa), the Seebeck coefficient becomes smaller with higher doping level, in agreement with theoretical findings. These facts overwhelm the positive influence of Te on the thermal conductivity. A further effect of the Te substitution is the shift of the maximum magnitude of S to lower temperatures.

All these effects combine to yield a maximum ZT value of 0.65 at 680 K for optimal dopings of 2.0 at. % and 0.75 at. % for Ni and Te, respectively. Higher temperature could even improve this promising maximum ZT value.

VII. CONCLUSION

Nanostructured $CoSb_3$ skutterudite material with partial substitution of Co by Ni and Sb by Te, respectively, has been prepared at moderate temperatures to obtain a high concentration of grain boundaries in the final pellet, which scatters phonons at a higher rate than electrons, thus resulting in a lower thermal conductivity.

The structure of the material has been investigated by SEM, AFM, and XRD revealing grain sizes from 175 up to 250 nm, and impurities of $CoSb_2$ and Sb phases up to 4%. The theoretical predictions for the best doping level of $Co_{1-x}Ni_xSb_{3-x}Te_x$ agree with experiment. Evaluation of the thermoelectric properties has been performed to find the most suitable combination of Te and Ni substitutions. The tested combinations give a best Ni and Te substitution of 2.0 at. % and 0.75 at. %, respectively, with a ZT value of 0.65 at 680 K.

ACKNOWLEDGMENTS

This work was supported by European Community under contract number G5RD-CT2000-00292, NanoThermel project. Special thanks go to all partners in this project, A. Saramat and A. Palmqvist (Chalmers University of Technology, Goteborg, Sweden), G. Noriega (CIDETE, Spain), and L. Holmgren (LEGELAB, Sweden).

[1]G. A. Slack, in *CRC Handbook of Thermoelectrics*, edited by D. M. Rowe (CRC Press, Boca Roton, Florida, 1995), p. 407–440.
[2]M. Christensen, L. Bertini, M. Toprak, E. Nishibori, M. Muhammed, C. Gatti, and B. B. Iversen, J. Appl. Phys. **96**, 3148 (2004).
[3]K. Wojciechowsky, MRS Bull. **37**, 2023 (2002).
[4]L. Bertini, C. Stiewe, M. Toprak, S. Williams, D. Platzek, Y. Zhang, C. Gatti, E. Mueller, M. Muhammed, and M. Rowe, J. Appl. Phys. **93**, 438 (2003).
[5]L. Bertini *et al.*, in *Proc. of the 22nd Int. Conf. on Thermoelectrics*, La Grande Motte, France, 2003, edited by H. Scherrer and J. C. Tedenac (IEEE, Piscataway, NJ, 2003), pp. 85–88.
[6]J. S. Dyck, W. Chen, J. Yang, G. P. Meisner, and C. Uher, Phys. Rev. B **65**, 115204 (2002).
[7]K. Wojciechowski, J. Toboła, and J. Leszczyński, J. Alloys Compd. **361**, 19 (2003).
[8]J. S. Dyck, W. Chen, C. Uher, L. Chen, X. Tang, and T. Hirai, J. Appl. Phys. **91**, 3698 (2002).
[9]M. Toprak, Y. Zhang, M. Muhammed, A. A. Zakhidov, R. H. Baughman, and I. Khayrullin, in *Proc. of the 18th Int. Conf. on Thermoelectrics*, Baltimore, MD 1999, edited by J. Sharp, H. J. Goldsmid, and G. Nolas (IEEE, Piscataway, NJ, 2000), pp. 382–385.
[10]C. Stiewe, M. Toprak, D. Platzek, Y. Zhang, E. Müller, and M. Muhammed, *Proc. VIth European Workshop on Thermoelectrics*, 2001, Freiburg, Germany, Fraunhofer Institut Physikalische Messtechnik.
[11]V. R. Saunders, R. Dovesi, C. Roetti, M. Causá, N. M. Harrison, R. Orlando, and C. M. Zicovich-Wilson, *CRYSTAL98, User's Manual*, University of Torino, Torino, 1998.
[12]A. D. Becke, J. Chem. Phys. **98**, 5648 (1993); J. P. Perdew and Y. Wang, Phys. Rev. B **40**, 3399 (1989).
[13]W. R. Wadt and P. J. Hay, J. Chem. Phys. **82**, 284 (1985).
[14]P. J. Hay and W. R. Wadt, J. Chem. Phys. **82**, 299 (1985).
[15]http://www.emsl.pnl.gov/forms/basisform.html
[16]LoptCG (Shell Procedure for numerical gradient optimizations) written and developed by C. M. Zicovich-Wilson, Instituto de Tecnología Química, UPS-CSIC, Spain, 1998.
[17]L. Bertini and C. Gatti (unpublished).
[18]S. Elliott, *The Physics and Chemistry of Solids* (Wiley, New York, 1998).
[19]N. P. Blake, S. Latturner, J. D. Bryan, G. D. Stucky, and H. Metiu, J. Chem. Phys. **115**, 8060 (2001).
[20]L. Bertini and C. Gatti, J. Chem. Phys. **121**, 8983 (2004).
[21]G. S. Nolas, D. T. Morelli, and T. M. Tritt, Annu. Rev. Mater. Sci. **29**, 89 (1999).
[22]K. T. Wojciechowski, J. Tobola and J. Leszczynski, J. Alloys Compd. **361**, 19 (2003).
[23]M. Toprak, C. Stiewe, D. Platzek, S. Williams, L. Bertini, E. Müller, C. Gatti, Y. Zhang, M. Rowe, and M. Muhammed, Adv. Funct. Mater. (in press).
[24]Preliminary results are reported in L. Bertini *et al.*, in *Proc. of the 22nd Int. Conf. on Thermoelectrics*, La Grande Motte, France 2003, edited by H. Scherrer and J. C. Tedenac (IEEE, Piscataway, NJ, 2003), pp. 48–51.
[25]L. Bertini *et al.*, in *Proc. of the 22nd Int. Conf. on Thermoelectrics*, La Grande Motte, France 2003, edited by H. Scherrer and J. C. Tedenac (IEEE, Piscataway, NJ, 2003), pp. 93–96.